ELSEVIER

Journal of Organometallic Chemistry 529 (1997) 395–408

Journal of Organometallic Chemistry

[2 + 2] Photocycloadditions of $[(\eta^5\text{-}C_5H_5)Ru(DMPP)_2L]PF_6$ complexes

Hong-li Ji [a], John H. Nelson [a,*], Andre DeCian [b], Jean Fischer [b], Bin Li [c], Chong Wang [c], Baryn McCarty [c], Yuri Aoki [c], John W. Kenney III [c], Ljiljana Solujic' [a], Emil B. Milosavljevic' [a]

[a] *Department of Chemistry, University of Nevada, Reno, NV 89557, USA*
[b] *Laboratoire de Cristallochimie et de Chimie Structurale (URA424-CNRS), University Louis Pasteur, 67070 Strasbourg Cedex, France*
[c] *Department of Physical Sciences, Eastern New Mexico University, Portales, NM 88130, USA*

Received 24 April 1996; revised 24 September 1996

Abstract

A series of $[(\eta^5\text{-}C_5H_5)Ru(DMPP)_2L]PF_6$ complexes, DMPP = 1-phenyl-3,4-dimethylphosphole, L = CH_3CN, Ph_3P, $PhS(O)_2CH{=}CH_2$, $(CH_3)_2NC(O)CH{=}CH_2$, $PhN{\equiv}C$, CO and $(CH_3O)_3P$, was found to undergo sunlight initiated [2 + 2] photodimerization of the coordinated phospholes only when L is a good π-acceptor ligand. These [2 + 2] dimerizations are accompanied by [4 + 2] dimerizations. The ratio of the [2 + 2] to [4 + 2] cycloaddition products is a function of the steric bulk of L. The nature of the photoexcited state has been probed by electron absorption and emission spectroscopy. The electron absorption spectra show high ε bands in the near UV region that are attributed to DMPP $\pi \rightarrow \pi^*$ transitions. The emission spectral lifetimes are a function of L and their magnitude at 77 K (about 0.2 to 2.0 μs), together with large Stokes shifts, is indicative of phosphorescence from a triplet excited state. It is postulated that this triplet excited state undergoes cycloaddition by way of a biradical intermediate. The complexes have been characterized by elemental analyses, infrared, electronic, and ^1H, $^1H\{^{31}P\}$, $^{13}C\{^1H\}$ and $^{31}P\{^1H\}$ NMR spectroscopy and cyclic voltammetry. The structure of $\{(\eta^5\text{-}C_5H_5)Ru(DMPP)_2[2+2](CO)\}PF_6$ was confirmed by X-ray crystallography. The complex cation possesses a non-crystallographic mirror plane, the two Ru–P distances (2.282(1) and 2.281(2) Å) are equivalent and the cyclobutane ring has a long (1.607(8) Å) and a short (1.550(8) Å) C–C bond.

Keywords: Phosphole; [2 + 2] Photocycloaddition

1. Introduction

This research was prompted by the previous results of Mathey and coworkers [1] who reported intramolecular [2 + 2] and [4 + 2] photodimerization of phospholes within the coordination spheres of Cr(0), Mo(0) and W(0) carbonyl complexes. These authors concluded that the [4 + 2] cycloaddition products were formed by thermal rearrangement of the primary [2 + 2] photocycloaddition products (Scheme 1).

Their conclusions were based upon indirect evidence, because the [2 + 2] cycloaddition product from reactions of DMPP could neither be isolated nor spectroscopically observed. However, their hypothesis was strongly supported by their isolation of the [2 + 2] cycloaddition product from the reaction of 1-phenylphosphole with molybdenum hexacarbonyl under UV irradiation (reaction 1) and the thermal rearrangement of the [2 + 2] photodimer in the presence of elemental sulfur (reaction 2). Reaction 2 is believed to involve the [4 + 2] dimer as an intermediate which undergoes a retro Diels–Alder reaction eliminating the phosphinidine [2] "PhP". The resulting phosphindole is then oxidatively displaced from molybdenum to produce the phosphindole sulfide. These observations lead to the following obvious questions. Why did the *cis*-$(DMPP)_2M(CO)_4$ complexes not undergo thermal intramolecular [4 + 2] Diels–Alder reactions? Why were the [2 + 2] cycloaddition products not observed in the reaction illustrated in Scheme 1? Why did the [2 + 2] products of reaction 1 not thermally rearrange to the [4 + 2] products in the absence of sulfur?

* Corresponding author.

PII S0022-328X(96)06817-9

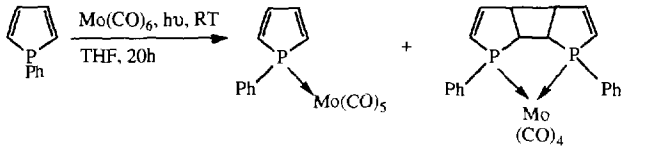

(1)

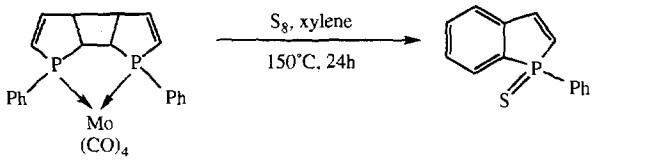

(2)

In the course of the synthesis of half-sandwich chiral ruthenium complexes via intramolecular [4 + 2] cycloadditions of DMPP with various dienophiles, a series of bis-DMPP complexes $[(\eta^5\text{-}C_5H_5)Ru(DMPP)_2L]PF_6$ was synthesized [3]. Most of them underwent [4 + 2] cycloadditions at elevated temperatures when L was a good dienophile. However, neither [4 + 2] nor [2 + 2] cyclodimerization of DMPP occurred either thermally or photochemically. These observations are easy to rationalize when L is diphenylvinylphosphine (DPVP), divinylphenylphosphine (DVPP), 2-vinylpyridine, phenylvinylsulfoxide or diallylphenylphosphine (DAPP), because all of these ligands are better dienophiles than DMPP. However, these observations are harder to explain when the ligands are acetonitrile, N,N-dimethylacrylamide, phenylvinylsulfone, triphenylphosphine, *tris*-(phenylethynyl)phosphine, etc., because in these latter cases neither Diels–Alder reactions nor [2 + 2] cyclodimerization of the two DMPP ligands was observed. Comparison of these results with those of Mathey and coworkers [1] suggested that good π-acceptor ligands, like CO, may play a great role in promoting the photochemical reactions of coordinated DMPP. Consequently, a series of $[(\eta^5\text{-}C_5H_5)Ru(DMPP)_2L]PF_6$ complexes with L of varying π-acceptor ability was prepared, and their photochemistry investigated. The results of these studies are described herein.

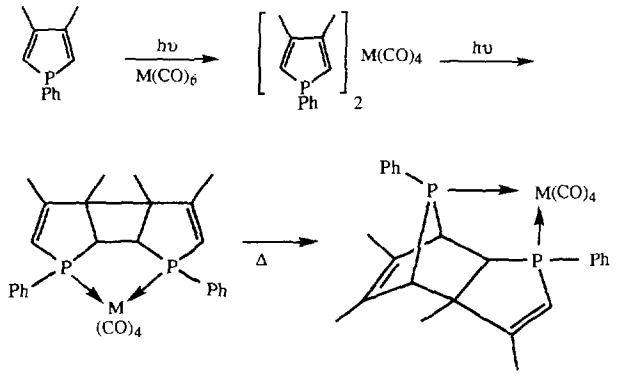

Scheme 1. Proposed mechanism [1] of Diels–Alder dimerization of 1-phenyl-3,4-dimethylphosphole within the coordination sphere of Group 6B metal tetracarbonyl moieties.

2. Results

Acetonitrile is readily thermally displaced from the substitutionally labile complex $[(\eta^5\text{-}C_5H_5)Ru(DMPP)_2(CH_3CN)]PF_6$ by a wide variety of ligands [3]. These reactions proceed in good yield to produce yellow crystalline solids when performed in the dark. Solutions of $[(\eta\text{-}C_5H_5)Ru(DMPP)_2L]PF_6$, L = CO, PhN≡C, DMPP and $(CH_3O)_3P$ are very light sensitive and undergo both [2 + 2] and [4 + 2] cyclodimerizations of the two coordinated DMPP ligands when exposed to ambient light in Pyrex vessels (reaction 3) to produce colorless complexes.

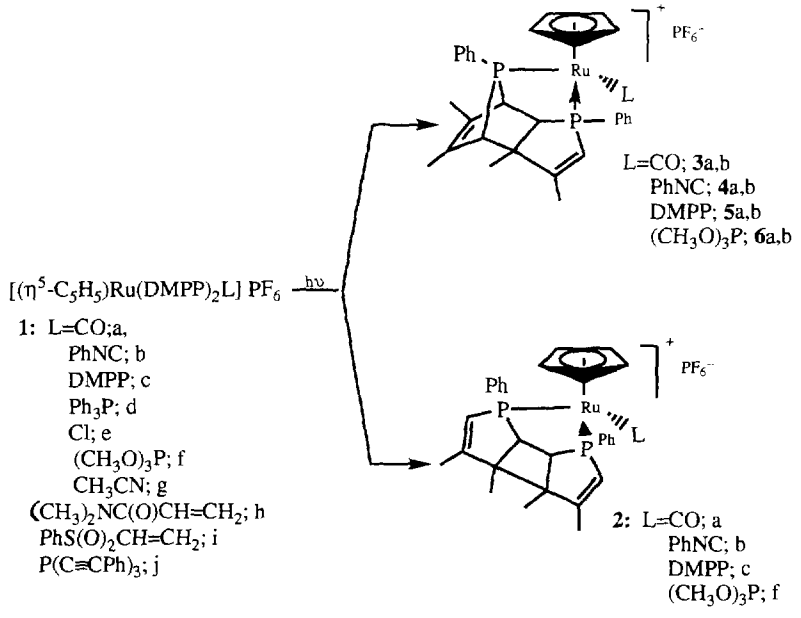

(3)

When L = CO, PhN≡C or $(CH_3O)_3P$, the [2 + 2] dimer is the major product; but when L = DMPP nearly equal amounts of the [2 + 2] and [4 + 2] products were formed, with the [4 + 2] product being slightly favored. Neither [2 + 2] nor [4 + 2] dimerizations occurred when L = CH_3CN, Ph_3P, Cl, $(CH_3)_2NC(O)CH=CH_2$, $PhS(O)_2CH=CH_2$ or $P(C\equiv CPh)_3$.

New complexes were characterized by infrared and NMR spectroscopy. The ν_{CO} vibration of $[(\eta^5\text{-}C_5H_5)Ru(DMPP)_2(CO)]PF_6$ (**1a**) decreased from 1990 to 1975 cm^{-1} on forming the [2 + 2] cycloaddition product **2a**. Similarly, the ν_{NC} vibration of $[(\eta^5\text{-}C_5H_5)Ru(DMPP)_2(PhNC)]PF_6$ (**1b**) decreased from 2230 to 2215 cm^{-1} on forming the [2 + 2] cycloaddition product **2b**. This 15 cm^{-1} reduction in the energies of ν_{CO} and ν_{NC} indicates an increased σ-donor ability of the [2 + 2] chelating diphosphadiene relative to two modentate DMPP ligands.

The ^{31}P chemical shift moves significantly downfield from about 44 to 106 ppm upon formation of the [2 + 2] cycloadducts. This large downfield shift results from the combined effects of a five-membered chelate ring [4] and the ring strain arising from the formation of the four-membered ring [5]. A single phosphorus resonance for the chelating diphosphadiene indicates that its two phosphorus nuclei are symmetry related. The ^1H and $^{13}C\{^1H\}$ NMR spectra of the [2 + 2] cycloadducts show second order multiplets confirming this fact [6]. The structure of carbonyl-5-cyclopentadienyl(1,4-diphenyl-1,4-diphospha-6,7,8,9-tetramethyltricyclo [5,4,^{2,8}0,^{3,7}] deca 5,9-diene) ruthenium(II) hexafluorophosphate (**2a**) was confirmed by X-ray crystallography (Fig. 1). Final atom coordinates are given in Table 1, and selected bond distances and angles in Tables 2 and 3 respectively. The structure consists of isolated cations and anions with no short contacts. The cation has distorted octahedral piano-stool geometry. The diphosphine ligand and possesses a non-crystallographic mirror plane which passes through the center of the cyclobutane ring. The two phosphorus donors are equidistant from ruthenium (2.282(1) and 2.281(2) Å). The cyclobutane ring is essentially planar, but not square. The C4–C5 distance (1.550(7) Å) is slightly shorter and the C3–C6 distance (1.607(8) Å) significantly longer than the average C–C distance within the ring of 1.558 ± 0.033 Å. The angles

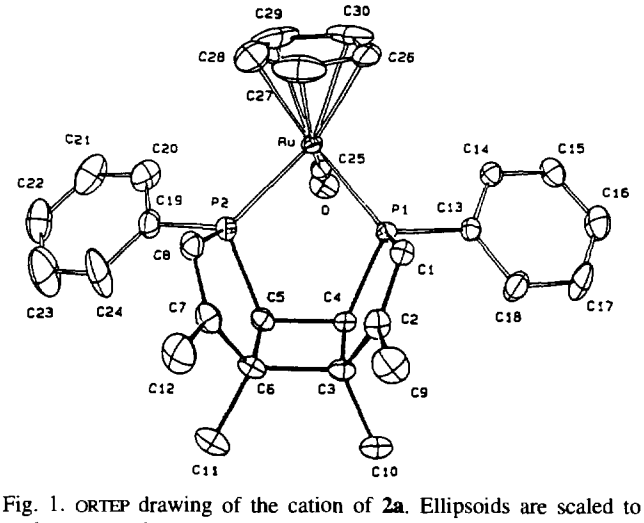

Fig. 1. ORTEP drawing of the cation of **2a**. Ellipsoids are scaled to enclose 50% of the electronic density. Hydrogen atoms are omitted.

Table 1
Atom coordinates for **2a** [a]

Atom	x	y	z	B (Å²)
Ru	0.29802(2)	0.20548(5)	0.10704(4)	3.08(1)
Cl1	0.8848(1)	0.4224(5)	0.2460(3)	13.0(1)
Cl2	0.8117(2)	0.5969(5)	0.2187(4)	15.5(1)
Cl3	−1.0070(2)	0.2196(6)	0.3727(6)	19.7(2)
Cl4	−0.9368(3)	0.3781(7)	0.4716(7)	25.0(3)
P1	0.32536(6)	0.2250(2)	0.3044(2)	2.86(3)
P2	0.36624(6)	0.3047(2)	0.0993(2)	3.51(4)
P3	0.39117(8)	0.7390(2)	0.4193(2)	5.25(5)
F1	0.3679(3)	0.6461(6)	0.3381(9)	15.9(3)
F2	0.3864(5)	0.8233(8)	0.3174(8)	16.4(4)
F3	0.3438(3)	0.7850(7)	0.437(1)	15.8(3)
F4	0.4394(2)	0.6975(8)	0.4046(9)	14.0(3)
F5	0.4140(3)	0.8365(8)	0.5043(8)	13.7(3)
F6	0.3942(5)	0.657(1)	0.5191(8)	19.4(4)
O	0.2442(2)	0.4288(5)	0.1062(5)	5.9(1)
C1	0.3695(2)	0.1238(6)	0.3725(6)	3.4(1)
C2	0.4112(3)	0.1713(6)	0.4158(7)	4.0(2)
C3	0.4151(2)	0.3013(6)	0.4027(6)	3.6(2)
C4	0.3665(2)	0.3476(6)	0.3394(6)	3.0(1)
C5	0.3881(2)	0.3875(6)	0.2331(6)	3.5(2)
C6	0.4374(2)	0.3420(7)	0.2922(7)	4.0(2)
C7	0.4511(2)	0.2460(7)	0.2148(7)	4.2(2)
C8	0.4194(3)	0.2219(7)	0.1167(7)	4.3(2)
C9	0.4529(3)	0.1048(9)	0.4853(8)	6.4(2)
C10	0.4358(3)	0.3601(8)	0.5211(7)	5.5(2)
C11	0.4772(3)	0.4333(8)	0.3207(9)	6.1(2)
C12	0.4999(3)	0.188(1)	0.2442(9)	6.9(3)
C13	0.2822(2)	0.2307(6)	0.3992(6)	3.4(1)
C14	0.2335(3)	0.2126(7)	0.3548(7)	4.3(2)
C15	0.2006(3)	0.2096(8)	0.4275(8)	5.5(2)
C16	0.2164(3)	0.2244(9)	0.5461(8)	6.8(2)
C17	0.2631(4)	0.247(1)	0.5911(7)	7.8(3)
C18	0.2966(3)	0.251(1)	0.5187(7)	6.1(2)
C19	0.3676(3)	0.3979(8)	−0.0275(7)	5.1(2)
C20	0.3293(4)	0.4109(9)	−0.1128(8)	6.9(3)
C21	0.3323(5)	0.481(1)	−0.2110(9)	9.6(3)
C22	0.3748(5)	0.538(1)	−0.2182(9)	9.8(3)
C23	0.4133(5)	0.528(1)	−0.128(1)	12.9(4)
C24	0.4077(4)	0.456(1)	−0.037(1)	11.7(3)
C25	0.2646(2)	0.3421(7)	0.1075(6)	3.7(2)
C26	0.2747(5)	0.0227(8)	0.1103(8)	9.4(3)
C27	0.3150(4)	0.0264(8)	0.059(1)	9.6(3)
C28	0.3043(5)	0.083(1)	−0.032(1)	10.9(3)
C29	0.2644(6)	0.118(1)	−0.0539(9)	11.1(4)
C30	0.2397(3)	0.0823(9)	0.037(1)	9.6(3)
C31	0.8479(6)	0.522(1)	0.155(1)	16.5(5)
C32	−0.9681(8)	0.313(2)	0.353(2)	21.0(7)

[a] Anisotropically refined atoms are given in the form of the isotropic equivalent displacement parameter defined as $(4/3)[a^2\beta(1,1) + b^2\beta(2,2) + c^2\beta(3,3) + ab(\cos\gamma)\beta(1,2) + ac(\cos\beta)\beta(1,3) + bc(\cos\alpha)\beta(2,3)]$.

Table 2
Selected bond distances (Å) for **2a** [a]

Atom 1	Atom 2	Distance	Atom 1	Atom 2	Distance
Ru	P1	2.282(1)	O	C25	1.161(9)
Ru	P2	2.281(2)	C1	C2	1.322(9)
Ru	C25	1.846(8)	C2	C3	1.52(1)
Ru	C26	2.22(1)	C3	C4	1.537(9)
Ru	C27	2.22(1)	C3	C6	1.61(1)
Ru	C28	2.18(1)	C4	C5	1.55(1)
Ru	C29	2.18(1)	C5	C6	1.538(9)
Ru	C30	2.224(9)	C6	C7	1.53(1)
P1	C1	1.789(7)	C7	C8	1.34(1)
P1	C4	1.838(7)	C26	C27	1.40(2)
P1	C13	1.806(8)	C26	C30	1.37(1)
P2	C5	1.828(7)	C27	C28	1.23(2)
P2	C8	1.774(8)	C28	C29	1.19(2)
P2	C19	1.829(9)	C29	C30	1.44(2)

[a] Numbers in parentheses are estimated standard deviations in the least significant digit.

within the cyclobutane ring are not equal with those proximate to ruthenium (90.8(4) and 91.3(4)°), being slightly larger than those distal from ruthenium (89.1(4) and 88.7(4)°). The two phosphole rings are *syn*, with a dihedral angle between their planes of about 50°. The three fused rings are connected in a tub fashion with the four-membered ring being the bottom of the tub. The C7–C8 (1.340(9) Å) and C1–C2 (1.322(8) Å) distances are typical for C=C double bonds.

Table 3
Selected bond angles (°) for **2a** [a]

Atom 1	Atom 2	Atom 3	Angle	Atom 1	Atom 2	Atom 3	Angle
P1	Ru	P2	81.88(7)	C2	C3	C6	114.7(6)
P1	Ru	C25	89.5(2)	C2	C3	C10	111.8(6)
P1	Ru	C26	97.1(2)	C4	C3	C6	88.7(5)
P1	Ru	C27	107.1(3)	P1	C4	C3	108.6(5)
P1	Ru	C28	138.1(3)	P1	C4	C5	113.0(4)
P1	Ru	C29	156.1(3)	C3	C4	C5	91.3(5)
P1	Ru	C30	121.0(3)	P2	C5	C4	113.3(4)
P2	Ru	C25	91.0(2)	P2	C5	C6	109.5(5)
P2	Ru	C26	137.9(3)	C4	C5	C6	90.8(5)
P2	Ru	C27	103.2(3)	C3	C6	C5	89.1(5)
P2	Ru	C28	96.0(3)	C3	C6	C7	116.2(6)
P2	Ru	C29	116.2(4)	C3	C6	C11	114.8(6)
P2	Ru	C30	153.6(3)	C5	C6	C7	107.7(6)
C1	P1	C4	92.2(3)	C5	C6	C11	115.9(6)
C1	P1	C13	105.2(3)	C7	C6	C11	111.2(7)
C4	P1	C13	108.8(3)	C6	C7	C8	116.2(6)
C5	P2	C8	92.3(3)	C6	C7	C12	120.9(7)
C5	P2	C19	108.4(4)	C8	C7	C12	122.7(8)
C8	P2	C19	105.0(4)	P2	C8	C7	114.2(6)
P1	C1	C2	113.9(5)	P1	C13	C14	121.2(5)
C1	C2	C3	116.9(6)	P1	C13	C18	120.4(6)
C1	C2	C9	123.5(7)	C4	C3	C10	115.3(6)
C3	C2	C9	119.4(6)	C6	C3	C10	115.8(6)
C2	C3	C4	108.4(5)	Ru	C25	O	178.7(7)

[a] Numbers in parentheses are estimated standard deviations in the least significant digit.

Comparison of the bond distances Ru–P (2.281(1) Å) and Ru–CO (1.846(7) Å) of complex **2a** with those of $[(\eta^5\text{-}C_5H_5)Ru(DPVP)_2(CO)]PF_6$ [7], Ru–P (2.322(1) Å) and Ru–CO (1.867(5) Å), indicates that the chelating diphosphadiene is a much better donor than two monodentate DPVP ligands.

3. Discussion

3.1. Diastereoselectivity of DMPP cycloadditions

These [2 + 2] and [4 + 2] cyclodimerizations do not occur in the absence of a suitable transition metal. If they were to occur, four isomers of the [2 + 2] dimer and two isomers of the [4 + 2] dimer could form, as illustrated in Scheme 2.

Coordination of the two DMPP ligands to a transition metal provides molecular direction and electronic activation in a highly organized transition state. Only the *syn*, head-to-head isomer forms in the [2 + 2] dimerization and only the *syn–exo* isomer forms in the [4 + 2] dimerization. Thus, the [2 + 2] cycloaddition yields a *meso* ligand and, of the two possible diastereomers about ruthenium (A and B) shown below, only A is formed because of the severe destabilizing intramolecular steric repulsions that would be obtained for diastereomer B.

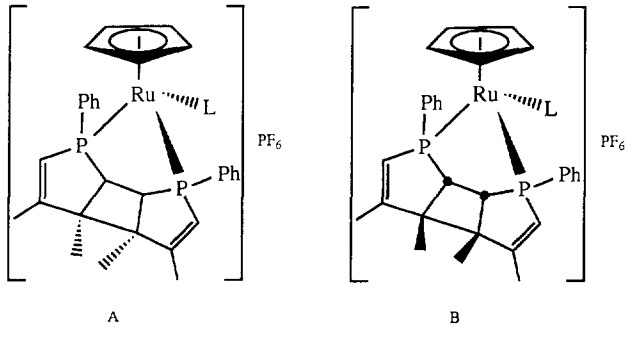

A B

The situation is different for the [4 + 2] cycloadduct, because it is an asymmetric bidentate ligand. Intramolecular Diels–Alder cycloadditions are known to be highly diastereoselective [8]. Only two ruthenium complexes, each as a racemic mixture of two enantiomers, are possible for this asymmetric ligand, as illustrated by C–F below. These diastereomers differ both in their absolute configurations at ruthenium and in the bidentate ligands, which contain six stereocenters. All diastereomers were obtained in these reactions in relative amounts that are a function of L.

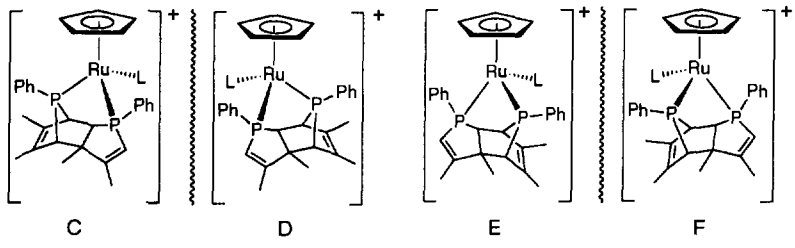

When L = CO the two pairs of racemates were formed in equal amounts, when L = PhN≡C the ratio of the two racemates was 2:1, when L = DMPP the ratio of the racemates was 4:1, and when L = $(CH_3O)_3P$ the ratio was 1:1. Thus, the ratio is a function of the asymmetry of the ligand L.

From a previously established empirical rule [9], it is believed that for complexes of the general formula $[(\eta^5\text{-}C_5H_5)Ru\{Ph_2PCH(CH_3)CH_2PPh_2\}X]$ the diastereomers having S_{Ru}, R_L configuration exhibit a difference in the ^{31}P chemical shifts for the two phosphorus nuclei which is always greater than that for the R_{Ru}, R_L diastereomer. [Absolute configurations were assigned according to the Baird–Sloan modification of the Cahn–Ingold–Prelog priority rules, see Ref. [10].] We have observed the same phenomenon for a number of analogous complexes [11]. On this basis we conclude that **4b**, **5b** and **6c** all possess the S_{Ru}, R_L and R_{Ru}, S_L configurations.

3.2. Proposed mechanism for the photochemical cycloadditions of $[(\eta^5\text{-}C_5H_5)Ru(DMPP)_2L]PF_6$

Mathey and coworkers [1] proposed that in the photochemical reactions of $(DMPP)_2M(CO)_4$ (M = Cr, Mo, W) the [4 + 2] cycloadducts were formed by thermal rearrangement of the initial [2 + 2] photoproducts. In order to ascertain whether this is the case for the ruthenium reactions, the isolated [2 + 2] cycloadducts were heated at 147 °C in 1,1,2,2-tetrachloroethane solutions and in sealed ampoules up to their melting points. No conversions to the [4 + 2] adducts occurred under these conditions, implying that the [2 + 2] and [4 + 2] cycloadducts were formed from a common intermediate [12]. Moreover, thermolysis of the $[(\eta^5\text{-}C_5H_5)Ru(DMPP)_2L]PF_6$ complexes in the dark produced neither [2 + 2] nor [4 + 2] products.

The $^{31}P\{^1H\}$ NMR monitored experiments established that the photochemical reactions are kinetically controlled. The [2 + 2] and [4 + 2] cycloadducts were simultaneously formed in the initial step, and the ratio between them did not change during the course of the reactions (up to 30 days). The relative ratios of the [2 + 2] and the two [4 + 2] cycloadducts are a function of the nature of the ancillary ligand L, as indeed is the propensity for the cycloaddition to occur. With the smaller L = CO the [2 + 2] and the two [4 + 2] cycloadducts were formed in a 4.25:1:1 ratio; with L = PhN≡C the ratio was 8:2:1; with L = DMPP the ratio was 3:4:1; and with L = $(CH_3O)_3P$ the ratio was 6:1:1. The varying ratios of the [2 + 2] and [4 + 2] products suggest that the photoinduced reactions are kinetically controlled and that the diastereoselectivity is mainly affected by interligand steric interactions and metal template effects. A concerted [2 + 2] photocycloaddition is symmetry allowed, but a concerted [4 + 2] cycloaddition is not [8], suggesting that these reactions are not concerted. In order to rationalize the experimental observations, the biradical mechanism [13] illustrated in Scheme 3 is proposed. Following photoexcitation to the π^* state of coordinated DMPP, the polarized phosphole rings undergo a stepwise addition producing the doubly allyl stabilized biradical, which should be a relatively slow step. Intramolecular photocycloadditions have been extensively investigated [14], and it is well known that interactions between two chromophores are particularly favored when they are connected by chains with three intervening units [15]. In these complexes steric effects allow the two phosphole rings to interact preferentially in a face-to-face fashion. The first carbon–carbon bond is formed in a *syn* manner. Subsequently, the cycloadditions occur via radical–radical coupling, which is probably fast. Radical–radical coupling occurs by two competing pathways: collapse between C_2 and C'_2 gives the [2 + 2] products while collapse between C_2 and C'_4 or between C'_2 and C_4 gives the two [4 + 2] products.

It should be noted that the iron analog $[(\eta^5\text{-}C_5H_5)Fe(DMPP)_3]PF_6$ does not undergo similar cycloadditions [16], but the $(DMPP)_2PtX_2$ [17] and $(DMPP)_2PdX_2$ [18] complexes do undergo thermal [2 + 2] and [4 + 2] cycloadditions by biradical pathways.

3.3. Nature of the photoexcited states

A qualitative molecular orbital energy level diagram for the $[(\eta^5\text{-}C_5H_5)Ru(DMPP)_2L]PF_6$ complexes is shown in Fig. 2. It predicts that the lower energy electronic transitions should be d–d transitions, and at higher energies ligand to metal charge transfer (LMCT) and/or DMPP $\pi \rightarrow \pi^*$ transitions may occur. The absorption spectra of each of these complexes display an intense absorption (ε about 10^4) in the 40200 to

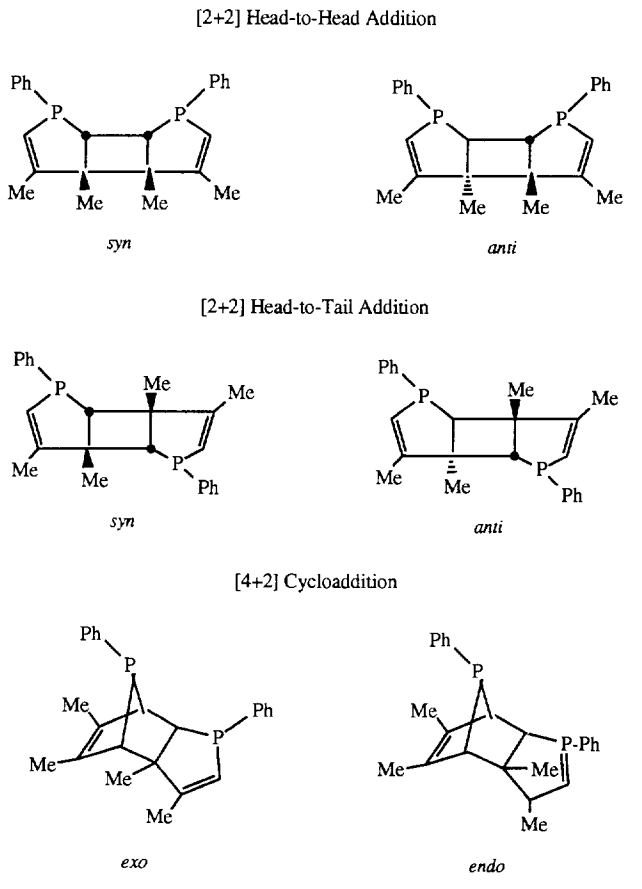

Scheme 2. Possible isomers resulting from cyclodimerization of DMPP.

43 800 cm^{-1} (228–240 nm) range that is probably a DMPP $\pi \rightarrow \pi^*$ and/or LMCT transition, and one or more resolved lower intensity bands (ε about 10^3) in the 27 000 to 38 000 cm^{-1} (258–370 nm) range that are probably d–d transitions. Typical absorption spectra are shown in Fig. 3. The emission spectra of the complexes are characterized by broad band widths with significant Stokes shifts from the absorbance maxima (Fig. 4). The magnitudes of the Stokes shifts and the luminescence lifetimes (0.2 to 2 μs, Table 4) suggest that the luminescence is due to phosphorescence [19].

Both the highest occupied molecular orbital (HOMO) and the lowest unoccupied molecular orbital (LUMO) are derived primarily from ruthenium d orbitals, but with some π character from the ligands. The emission is therefore associated with a standard HOMO ← LUMO one electron de-excitation process, essentially d-to-d in character, but subject to ligand perturbations via π interactions. From Fig. 2 it is seen that the luminescence transition at the electron configuration level is $[core](6a')^2 \leftarrow [core](6a')^1(7a')^1$, and at the state level $^1A' \leftarrow {}^3A'$. Changes in the energy of the HOMO as a function of L will result in changes in the HOMO–LUMO energy gap. This will affect both luminescence maxima and lifetimes. The complexes containing the less electron-releasing ligands [$(CH_3O)_3P$, PhN≡C, CO] all exhibit higher energy emissions (about 14 600 cm^{-1}), while for more electron-releasing ligands (DMPP, Br^-, Ph_3P) luminescence occurs at about 11 400 cm^{-1}. Luminescence lifetimes follow the general trend that a higher energy emission exhibits a somewhat longer lifetime than a lower energy emission.

The photochemical and photophysical properties of these $[(\eta^5\text{-}C_5H_5)Ru(DMPP)_2L]PF_6$ complexes can be explained in a consistent manner if the following assumptions are made. First, the exciting photons are assumed to activate the π systems of the coordinated DMPP. Second, the electronically excited DMPP* ligands have sufficient lifetimes to undergo interligand photochemistry. The conventional wisdom concerning [2 + 2] photocycloadditions is that they are most productive from triplet states that are biradical in nature [20]. Third, the energy transfer process from the excited DMPP* π orbitals to the metal d orbitals is comparatively inefficient, even at 77 K. Fourth, emission can occur both from the coordinated DMPP π-system and from the metal d system, as evidenced by the existence

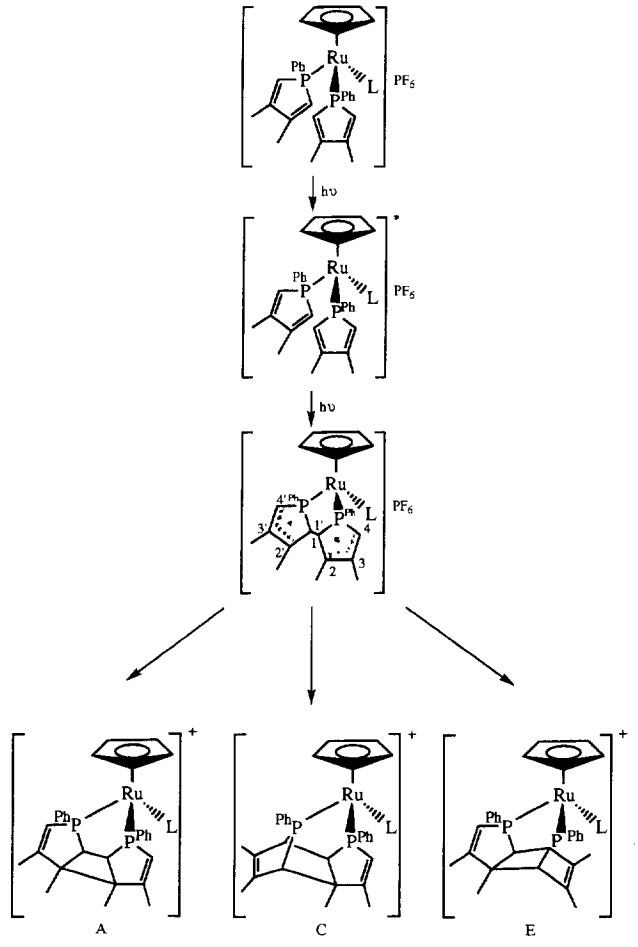

Scheme 3. Proposed mechanism for photochemically induced cycloadditions of $[(\eta^5\text{-}C_5H_5)Ru(DMPP)_2L]PF_6$ complexes.

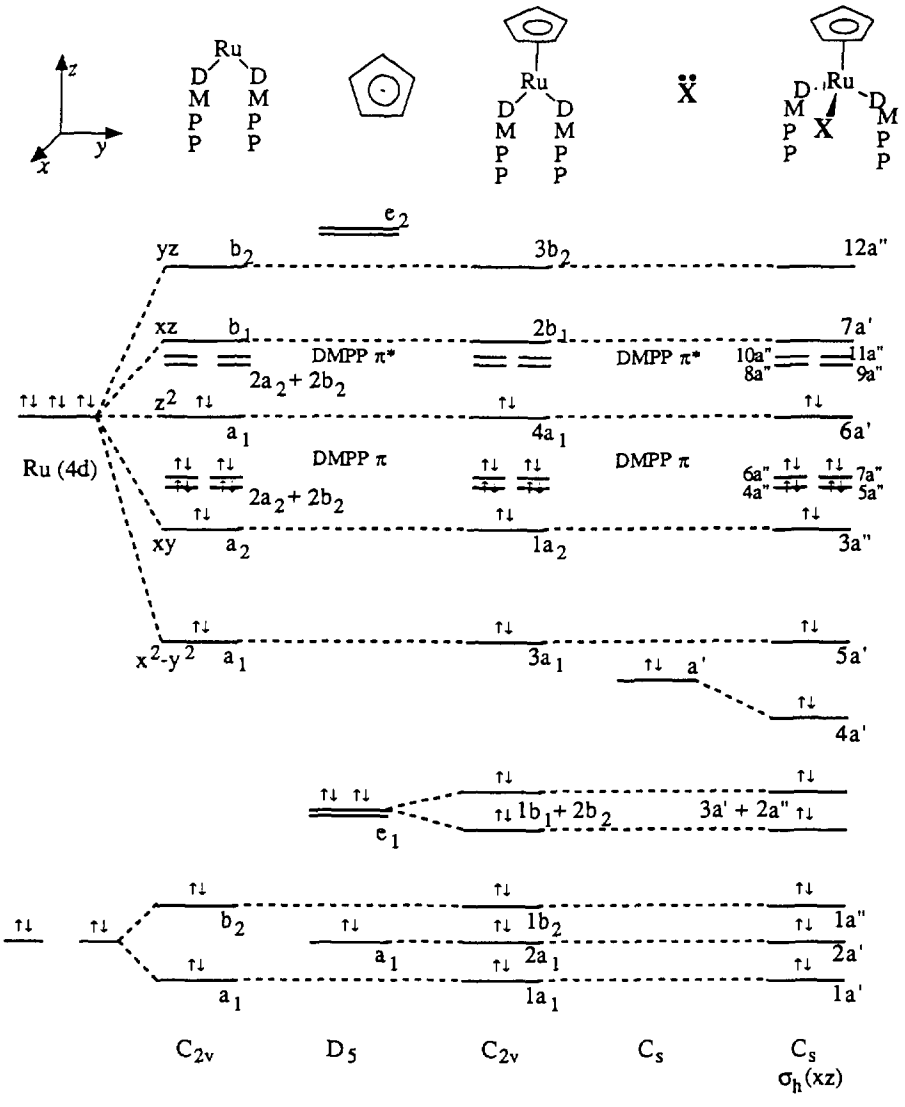

Fig. 2. Qualitative MO diagram for $[(\eta^5\text{-}C_5H_5)Ru(DMPP)_2L]^+$.

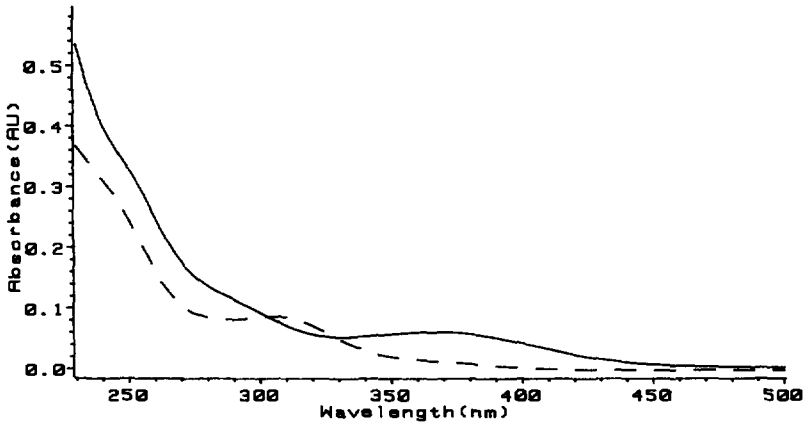

Fig. 3. Electronic absorption spectra of $[(\eta^5\text{-}C_5H_5)Ru(DMPP)_2L]PF_6$ in CH_3CN, 0.1 cm path length, L = CO (– – –) (1.48×10^{-4} M), bottom L = CH_3CN (————) (1.67×10^{-4} M).

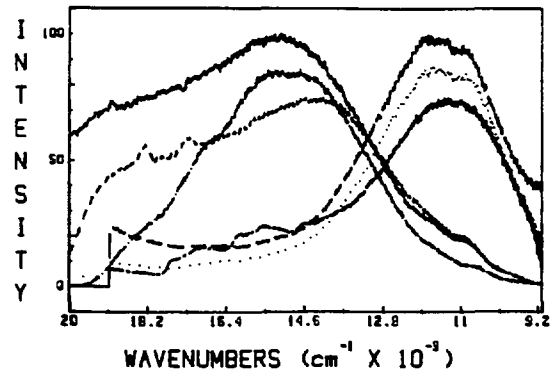

Fig. 4. Corrected luminescence of $[(\eta^5\text{-}C_5H_5)Ru(DMPP)_2L]PF_6$, $L = (CH_3O)_3P$ (————), PhN_3C (– · –), CO (– – –), DMPP (· · ·), Br(— — — —), and Ph_3P (– · –). These spectra were obtained from solid microcrystalline samples at 77 K using 27 400 cm^{-1} (365 nm) broad band near UV excitation from a mercury/xenon arc lamp. The luminescence band maxima of these complexes occur at 15 000, 14 800, 14 200, 11 809, 11 700 and 11 400 cm^{-1} respectively.

of distinct high and low energy emission ranges, and in some cases by broad mixed emissions. Fifth, the emission properties and the tendencies to undergo DMPP photodimerization are strongly influenced by the nature of the ancillary ligand L. Sixth, the σ-donor, π-donor/acceptor and steric properties of L govern the photochemistry and photophysics of these complexes.

These complexes represent interesting exceptions to the Crosby–Kasha rule [19]. If the Crosby–Kasha rule were obeyed, then all emissions would be the lower energy d–d metal centered emissions and the compounds would not undergo DMPP ligand photodimerizations. The relative efficiency of excitation energy transfer from the DMPP ligands to the metal center is clearly competitive with the efficiency of DMPP-centered photophysics and photochemistry, etc. and very sensitive to the nature of L.

3.4. Electrochemistry

It has been pointed out by several authors [21] that there is a good correlation between the redox potential of a complex and the energy of the charge transfer transition. For LMCT one thus expects that better donors will give rise to higher energy LMCT transitions and lower oxidation potentials. The redox properties of the complexes are listed in Table 5. For all complexes the redox couples are quasi-reversible one-electron processes with fast follow-up chemical steps, and in most cases no cathodic wave could be seen on the return sweep, even at high scan rates. The peak potential for the Ru(II)/Ru(III) couple ranged from 0.58 to 1.24 V, similar to what we have observed for other ruthenium(II) complexes [3,22]. The reduction potentials, where observable, are near −2.0 V. The ease of oxidation increases in the order $L = CH_3CN > (CH_3)_2NC(O)CH{=}CH_2 > PhN{\equiv}C > PhS(O)_2CH{=}CH_2$, and this correlates reasonably well with a decrease in the energy of the highest energy transitions, for which the order is $L = CH_3CN > CO > DMPP > (CH_3)_2NC(O)CH{=}CH_2 = PhS(O)_2CH{=}CH_2 >$

Table 4
Absorption [a] and luminescence [b] spectral data for the $[(\eta^5\text{-}C_5H_5)Ru(DMPP)_2L]PF_6$ complexes

L	Absorption	Luminescence	
	$\bar{\nu}_{max}$ (ε) ($cm^{-1} \times 10^3$ ($l\,mol^{-1}\,cm^{-1} \times 10^3$))	$\bar{\nu}_{max}$ ($cm^{-1} \times 10^3$)	τ (μs)
CH_3CN	41.7(22.9)(sh), 35.5(7.79)(sh), 27.2(3.62)	no emission	
CH_3CN^+	43.8(24.9), 27.0(3.36)		
$PhS(O)_2CH{=}CH_2$	43.9(43.6), 40.3(29.7)(sh), 34.2(7.95)(sh), 28.4(1.64)(sh)	12.4	not measured
$(CH_3)_2NC(O)CH{=}CH_2^+$	41.7(21.0), 28.7(4.3)	11.9	not measured
CO	44.2(26.4)(sh), 36.5(6.24)(sh), 32.9(5.81), 28.4(1.18)(sh)	14.2	0.40
CO^+	43.5(25.6), 32.3(6.13)		
PhNC	45.9(56.5)(sh), 41.7(31.4)(sh), 38.5(26.7)(sh), 31.4(8.64)(sh)	14.8	0.56
DMPP	42.7(25.2)(sh), 37.6(11.7)(sh), 33.9(7.07)(sh), 29.1(4.32)	11.8	0.21
$DMPP^+$	42.0(29.6), 38.5(sh), 33.3(sh), 28.6(4.38)		
Ph_3P	45.0(49.1)(sh), 40.3(22.7)(sh), 35.2(7.26)(sh), 27.9(3.12)	11.2	0.43
$(CH_3O)_3P$	41.7(18.5)(sh), 37.5(8.80)(sh), 33.3(4.81)(sh), 30.9(3.86)(sh), 27.3(1.36)(sh)	15.0	0.79
Br	42.0(17.4)(sh), 36.0(6.07)(sh), 33.3(4.43)(sh), 29.4(3.59)	11.7	0.29
CO[2 + 2]	44.2(40.0), 37.3(5.88), 30.9(0.99)(sh)	13.5	0.30
PhNC[2 + 2]	44.6(88.7), 36.5(20.5), 35.0(20.7), 30.3(5.80)(sh)	13.7	0.38
DMPP[2 + 2]	45.4(47.1)(sh), 40.7(20.5)(sh), 35.5(5.34)(sh), 30.5(3.85), 27.6(1.51)(sh)	13.6	0.33
DMPP[4 + 2]	45.9(48.1)(sh), 40.8(21.9)(sh), 35.7(7.01)(sh), 29.6(4.32), 27.1(1.99)(sh)	14.5	1.90
$(CH_3O)_3P$[2 + 2]	44.2(36.6), 38.2(6.47)(sh), 34.7(4.04), 30.3(2.12)(sh)	14.2	0.56

sh = shoulder.
[a] In N_2 or Ar saturated CH_3CN or $CH_2Cl_2^{(+)}$ solution at 289 K.
[b] As solids at 77 K.

Table 5
Redox characteristics of the $[(\eta^5\text{-}C_5H_5)Ru(DMPP)_2L]PF_6$ complexes [a]

L	Ep	
	Ru(II)/Ru(III)	Ru(II)/Ru(I)
CH_3CN	0.58 [b]	
$PhS(O)_2CH{=}CH_2$	1.23 [b]	−1.96 [c]
$Me_2NC(O)CH{=}CH_2$	0.81 [d]	
CO	—	−2.14 [c]
PhNC	0.89	—
CO[2+2]	1.24	—
PhNC[2+2]	E_{pa} 0.86	—
	E_{pc} 0.55	—

[a] In CH_2Cl_2 containing 0.1 M TBAP at 25 °C, $\nu = 200\,mV\,s^{-1}$. E values are vs. Fc^+/Fc.
[b] E_{pa} only.
[c] E_{pc} only.
[d] E_{max} determined by differential pulse voltammetry (peak oxidation potential could not be determined by cyclic voltammetry since it is too near the limit of the electrode/solvents/supporting electrolyte system used).

PhN≡C. This suggests that these transitions may not be pure DMPP $\pi \rightarrow \pi^*$ transitions, but may also possess some LMCT character.

3.5. Comparisons among the Cr, Mo, W, Ru, Pd and Pt promoted cycloadditions

The Cr, Mo and W complexes undergo photochemical [2 + 2] cyclodimerizations of DMPP, which are followed by irreversible thermal conversion to the [4 + 2] dimers [1]. For the platinum complexes, thermal dimerization occurs at 140 °C in both the solution and solid states [17]. Both the [2 + 2] and [4 + 2] dimers are in equilibrium with the biradical intermediate, and are ultimately quantitatively converted to the exomethylene product G by hydrogen atom transfer.

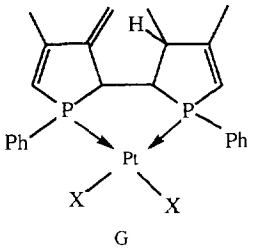

G

For the palladium complexes, thermal dimerization also occurs at 140 °C in both the solution and solid states [18]. In this case, the [4 + 2] dimer is formed first and thermally converted to the [2 + 2] dimer and exomethylene product. The ruthenium complexes undergo room temperature photochemical [2 + 2] and [4 + 2] phosphole dimerization and the [2 + 2] dimers are thermally stable. It was not possible to thermally convert them to either the [4 + 2] or exomethylene products at temperatures up to their decomposition points. We originally thought that the influence of the metal on the outcome of these reactions may be related to varying ring strain energies of the cyclobutane ring of the [2 + 2] dimers. A decrease in the P–M–P bite angle might be expected to result in increasing ring strain, signaled by an increase in the C–C bond distance within the cyclobutane ring for the bond remote from the metal. The P–Pt–P angle in the [2 + 2] dimer (86.1(1)°) [17] and the P–Pd–P angle in the [2 + 2] dimer (84.8(2)°) [18] are both larger than the R–Ru–P angle (81.88(7)°). The C–C distances within the cyclobutane ring for the bond remote from the metal complex for the platinum (1.59(2) Å) and palladium (1.617(25) Å) complexes are respectively shorter and the same length as the C–C distance for the ruthenium complex (1.61(1) Å). Clearly, there are other effects that are important in determining the relative thermal stabilities of the phosphole dimerization products.

4. Experimental

4.1. Reagents and physical measurements

Hydrated ruthenium trichoride (43.02% Ru, Johnson Matthey Aesar/Alfa), Ph_3P, $(CH_3O)_3P$, NH_4PF_6, CH_3CN, $(CH_3)_2NC(O)CH{=}CH_2$, $PhS(O)_2CH{=}CH_2$ (Aldrich) were used as received. $[(\eta^5\text{-}C_5H_5)Ru(DMPP)_2(CH_3CN))]PF_6$ [3] and PhN≡C [23] were prepared by literature procedures. All preparations involving phosphines were carried out under a dry nitrogen atmosphere. Specific precautions were taken during the preparation and isolation of the $[(\eta^5\text{-}C_5H_5)Ru(DMPP)_2(L)]PF_6$ complexes to avoid light. Photochemical reactions were performed using sunlight at ambient temperatures in dry solvents. Melting points were determined on a Mel-Temp apparatus and are uncorrected. Elemental analyses were performed by Galbraith Laboratories, Knoxville, TN 37921. Infrared spectra were obtained on a Perkin–Elmer 599 spectrometer. Cyclic voltammograms were recorded as previously described [22]. Electronic absorption and emission spectra were obtained as previously described [24]. $^{31}P\{^1H\}$ NMR spectra were recorded at 40.26 MHz on a JEOL FX-100 spectrometer in the FT mode or at 121.65 MHz on a General Electric GN-300 spectrometer. Phosphorus chemical shifts are relative to internal PF_6^- (−144.95 ppm), with a positive value being downfield of the reference. The ^1H, $^1H\{^{31}P\}$ and $^{13}C\{^1H\}$ spectra were recorded at 300, 300 and 75 MHz respectively, on a General Electric GN-300 spectrometer. Proton and carbon chemical shifts are relative to inter-

nal $(CH_3)_4Si$. Positive values are downfield of the reference.

4.2. Synthesis of $[(\eta^5\text{-}C_5H_5)Ru(DMPP)_2L]PF_6$ (1)

4.2.1. L = CO

CO gas was bubbled through a refluxing yellow–orange solution containing 0.70 g (0.96 mmol) $[(\eta^5\text{-}C_5H_5)Ru(DMPP)_2(CH_3CN))]PF_6$ in 30 ml CH_2Cl_2 in the dark for 4 h to give a clear yellow solution. The solution was cooled to ambient temperature, filtered through a short plug of silica gel and the solvent was removed on a rotary evaporator. The resulting solid was recrystalllized from $CHCl_3/(C_2H_5)_2O$ at low temperature to afford 0.62 g (90%) of yellow crystals of $[(\eta^5\text{-}C_5H_5)Ru(DMPP)_2(CO)]PF_6 \cdot CHCl_3$; m.p. 88 °C. IR (KBr): ν_{CO} 1990, $\nu_{(C_5H_5 \text{ and } PF_6^-)}$ 850 cm^{-1}. $^{31}P\{^1H\}$ NMR ($CDCl_3$): δ 39.84 (s, 2P, DMPP), −144.95 (septet, $^1J(PF) = 716$ Hz, 1P, PF_6^-). ^1H NMR ($CDCl_3$): δ 1.93 (s, 6H, CH_3), 2.00 (s, 6H, CH_3), 5.21 (s, 5H, C_5H_5), 6.26 (D, $|^2J(PH) + {}^4J(PH)| = 35.76$ Hz, 2H, H_α), 6.42 (D, $|^2J(PH) + {}^4J(PH)| = 35.76$ Hz, 2H, H_α), 7.25–7.40 (m, 10H, Ph). $^{13}C\{^1H\}$ NMR ($CDCl_3$): δ 17.31 (T, $|^3J(PC) + {}^5J(PC)| = 12.92$ Hz, CH_3), 87.87 (t, $^2J(PC) = 2.04$ Hz, C_5H_5), 127.11 (5L, $^1J(PC) = 56.88$, $^3J(PC) = -3.29$, $^2J(PP) = 23.89$ Hz, C_α), 127.66 (5L, $^1J(PC) = 52.18$, $^3J(PC) = 1.78$, $^2J(PP) = 23.89$ Hz, C_α), 128.97 (T, $|^3J(PC) + {}^5J(PC)| = 10.96$ Hz, C_m), 130.32 (5L, $^1J(PC) = 57.19$, $^3J(PC) = -345$ Hz, $^2J(PP) = 23.89$ Hz, C_i), 130.84 (s, C_p), 130.97 (T, $|^2J(PC) + {}^4J(PC)| = 11.11$ Hz, C_o), 151.11 (T, $|^2J(PC) + {}^4J(PC)| = 11.11$ Hz, C_β), 152.10 (T, $|^2J(PC) + {}^4J(PC)| = 10.13$ Hz, C_β), 200.40 (t, $^2J(PC) = 16.70$ Hz, CO). Anal. Found: C, 44.15; H, 3.88. $C_{31}H_{32}ClF_6OP_3Ru$ Calc.: C, 44.12; H, 3.82%.

4.2.2. L = PhN≡C

To a solution containing 0.3 g (0.41 mmol) $[(\eta^5\text{-}C_5H_5)Ru(DMPP)_2(CH_3CN)]PF_6$ in 20 ml 1,2-dichloroethane was added 0.3 ml (3.4 mmol) PhN≡C by syringe under N_2. After heating at reflux for 2 h in the dark the solvent was removed on a rotary evaporator and the oily residue was washed with anhydrous diethyl ether. Recrystallization from CH_2Cl_2/ether/pet ether (30–70 °C) gave a pale yellow crystalline solid which was dried under vacuum overnight. The yield is nearly quantitative; m.p. 206–208 °C. IR (KBr): ν_{CN} 2230, $\nu_{(C_5H_5 \text{ and } PF_6^-)}$ 850 cm^{-1}. $^{31}P\{^1H\}$ NMR ($CDCl_3$): δ 44.94 (s, 2P, DMPP), −144.95 (septet, $^1J(PF) = 716$ Hz, 1P, PF_6^-). ^1H NMR ($CDCl_3$): δ 1.89 (s, 6H, CH_3), 1.92 (s, 6H, CH_3), 5.15 (s, 5H, C_5H_5), 6.24 (D, $|^2J(PH) + {}^4J(PH)| = 34.26$ Hz, 2H, H_α), 6.31 (D, $|^2J(PH) + {}^4J(PH)| = 33.66$ Hz, 2H, H_α), 7.25–7.40 (m, 15H, Ph). $^{13}C\{^1H\}$ NMR ($CDCl_3$): δ 17.23 (T, $|^3J(PC) + {}^5J(PC)| = 13.38$ Hz, CH_3), 17.32 (T, $|^3J(PC) + {}^5J(PC)| = 13.53$ Hz, CH_3), 85.04 (s, C_5H_5), 125.38 (s, C'_i and C'_o), 128.42 (s, C'_p), 128.68 (T, $|^3J(PC) + {}^5J(PC)| = 10.51$ Hz, C_m), 128.78 (m, C_α), 129.97 (m, C_α), 129.65 (s, C'_m), 130.03 (m, C_i), 130.47 (s, C_p), 131.24 (T, $|^2J(PC) + {}^4J(PC)| = 11.11$ Hz, C_o), 149.60 (T, $|^2J(PC) + {}^4J(PC)| = 9.67$ Hz, C_β), 150.96 (T, $|^2J(PC) + {}^4J(PC)| = 9.22$ Hz, C_β), 161.67 (t, $^2J(PC) = 22.50$ Hz, CN). The primed carbons are the phenyl carbons of PhNC. Anal. Found: C, 54.50; H, 4.65. $C_{36}H_{36}NP_3F_6Ru$ Calc.: C, 54.69; H, 4.59%.

4.2.3. L = DMPP

Under a purge of N_2, 0.3 ml (1.60 mmol) of DMPP was added to a solution containing 1.0 g (1.37 mmol) $[(\eta^5\text{-}C_5H_5)Ru(DMPP)_2(CH_3CN))]PF_6$ in 50 ml of 1,2-dichloroethane. The solution was refluxed under N_2 in the dark overnight. The solvent was removed on a rotary evaporator and the residue was washed with anhydrous diethyl ether. Recrystallization from $CHCl_3/(C_2H_5)_2O$ at low temperature afforded 0.96 g (80%) of block-shaped shiny yellow crystals of $[(\eta^5\text{-}C_5H_5)Ru(DMPP)_3]PF_6$; m.p. 227–228 °C. $^{31}P\{^1H\}$ NMR ($CDCl_3$): δ 45.31 (s, 3P, DMPP), −144.95 (septet, $^1J(PF) = 716$ Hz, 1P, PF_6^-). ^1H NMR ($CDCl_3$): δ 1.61 (s, 18H, CH_3), 5.46 (s, 5H, C_5H_5), 6.27 (m, 6H, H_α), 7.00–7.40 (m, 15H, Ph). $^{13}C\{^1H\}$ NMR ($CDCl_3$): δ 16.85 (4 line $A[X]_3$ pattern, CH_3), 82.06 (s, C_5H_5), 128.22 (4 line, $A[X]_3$, C_m), 129.74 (s, C_p), 130.16 (m, $A[X]_3$, C_α), 130.62 (4 line $A[X]_3$, C_o), 150.43 (4 line, $A[X]_3$, C_β). Anal. Found: C, 52.49; H, 4.84. $C_{41}H_{44}F_6P_4Ru \cdot 0.5CHCl_3$ Calc.: C, 52.64; H, 4.79%.

4.2.4. $[(\eta^5\text{-}C_5H_5)Ru(DMPP)_2(ph_3P)]PF_6$

This compound was prepared similarly and isolated as a yellow powder in 90% yield. $^{31}P\{^1H\}$ NMR ($CDCl_3$): δ 36.88 (d, $^2J(PP) = 36.62$ Hz, 2P, DMPP), 46.03 (t, $^2J(PP) = 36.62$ Hz, 1P, Ph_3P), −144.95 (septet, $^1J(PF) = 716$ Hz, 1P, PF_6^-). Thermolysis in $ClCH_2CH_2Cl$ at 80 °C for 24 h or photolysis in $CHCl_3$ (sunlight, Pyrex flask at room temperature for 10 days) gave no detectable intramolecular [4 + 2] or [2 + 2] cycloaddition products.

4.2.5. L = Cl

To a solution containing 0.90 g (1.24 mmol) of $[(\eta^5\text{-}C_5H_5)Ru(DMPP)_2(CH_3CN))]PF_6$ in 30 ml of CH_2Cl_2 was added an aqueous solution containing 1.2 g (10.9 mmol) $(CH_3)_4NCl$. Then 95% ethanol was added until a single phase formed. After stirring the mixture for 4 h at ambient temperature, two products were present in solution: $[(\eta^5\text{-}C_5H_5)Ru(DMPP)_2(CH_3CN))]Cl$ (δ ^{31}P 46.78) and $[(\eta^5\text{-}C_5H_5)Ru(DMPP)Cl]$ (δ ^{31}P 46.29). The solvents were removed on a rotary evaporator and the residue was extracted with 1,2-dichloroethane. The extract was heated at reflux for 4 h and the solvent was removed on a rotary evaporator. The residue was dissolved in CH_2Cl_2 and the solution was passed

through a short silica gel column. The solvent was evaporated on a rotary evaporator and the residue was crystallized from $CHCl_3$/pet ether (70–110 °C) to produce $[(\eta^5\text{-}C_5H_5)Ru(DMPP)_2Cl]$ as a reddish crystalline solid in 70% yield. $^{31}P\{^1H\}$ NMR ($CDCl_3$): δ 46.29 (s). ^1H NMR ($CDCl_3$): δ 1.89 (s, 6H, CH_3), 1.94 (s, 6H, CH_3), 4.42 (s, 5H, C_5H_5), 6.16 (D, $|^2J(PH)+{}^4J(PH)|$ = 31.86 Hz, 2H, H_α), 6.46 (D, $|^2J(PH)+{}^4J(PH)|$ = 31.25 Hz, 2H, H_α), 7.20–7.60 (m, 10H, Ph). $^{13}C\{^1H\}$ NMR ($CDCl_3$): δ 17.54 (T, $|^3J(PC)+{}^5J(PC)|$ = 10.58 Hz, CH_3), 78.25 (t, $^2J(PC)$ = 3.30 Hz, C_5H_5), 127.76 (T, $|^3J(PC)+{}^5J(PC)|$ = 9.15 Hz, C_m), 128.85 (s, Cp), 129.27 (T, $|^1J(PC)+{}^3J(PC)|$ = 22.14 Hz, C_α), 131.12 (T, $|^1J(PC)+{}^3J(PC)|$ = 21.16 Hz, C_α), 131.58 (T, $|^2J(PC)+{}^4J(PC)|$ = 9.75 Hz, C_o), 135.72 (T, $|^1J(PC)+{}^3J(PC)|$ = 45.95 Hz, C_i), 146.76 (T, $|^2J(PC)+{}^4J(PC)|$ = 8.31 Hz, C_β), 148.39 (T, $|^2J(PC)+{}^4J(PC)|$ = 7.03 Hz, C_β). Thermolysis in $ClCH_2CH_2Cl$ at 80 °C for 24 h or photolysis in $CHCl_3$ (sunlight, Pyrex flask at room temperature for 10 days) gave no detectable intramolecular [4 + 2] or [2 + 2] cycloaddition products.

4.2.6. $L = (CH_3O)_3P$

This compound was prepared in the same manner as for L = PhN≡C from the reaction of 1.1 g of $[(\eta^5\text{-}C_5H_5)Ru(DMPP)_2(CH_3CN)]PF_6$ with 0.15 ml of $(CH_3O)_3P$ in 1,2-dichloroethane at 80 °C under N_2. The product was isolated as a yellow crystalline solid in quantitative yield. $^{31}P\{^1H\}$ NMR ($CDCl_3$): δ 150.0 (t, $^2J(PP)$ = 61.04 Hz, 1P, $(CH_3O)_3P$), 46.01, (d, $^2J(PP)$ = 61.04 Hz, 2P, DMPP), −144.95 (septet, $^1J(PF)$ = 713 Hz, PF_6^-).

4.3. Photoinduced cycloadditions of $[(\eta^5\text{-}C_5H_5)Ru(DMPP)_2L]PF_6$

4.3.1. $L = CO$

A solution containing 0.62 g of $[(\eta^5\text{-}C_5H_5)Ru(DMPP)_2(CO)]PF_6$ in 50 ml of dry $CHCl_3$ was exposed to sunlight for about 20 h. At this time the solution color changed from light yellow to deep orange and a white precipitate formed. The $^{31}P\{^1H\}$ NMR spectrum showed that a mixture of three compounds **2a**, **3a**, and **3b** had formed. The white precipitate (**2a**) was collected by filtration and washed with $CHCl_3$. The orange solution containing the three compounds was reduced in volume to about 10 ml and cooled to −14 °C, when a second crop of **2a** which precipitated was isolated by filtration. The filtrate still contained **2a**, **3a**, and **3b** in a 1:4:4 ratio, which was not further separated. The two crops of white crystalline solids were combined and recrystalllized from $CH_2Cl_2/CHCl_3$ at room temperature by slow evaporation to yield 0.42 g (68%) of **2a**; m.p. 121 °C decomp. IR (KBr): ν_{CO} 1975, $\nu_{(C_5H_5 \text{ and } PF_6^-)}$ 850 cm^{-1}. $^{31}P\{^1H\}$ ($CDCl_3$): δ 106.69 (s, 2P, (DMPP) [2 + 2]) −144.95 (septet, $^1J(PF)$ = 716 Hz, 1P, PF_6^-). ^1H NMR (CD_3NO_2): δ 1.74 (s, 6H, 2-CH_3), 2.04 (T, $|^4J(PH)+{}^6J(PH)|$ = 1.5 Hz, 6H, β-CH_3), 3.26 (m, $|^2J(PH)+{}^4J(PH)|$ = 18.03 Hz, 2H, H_1), 5.66 (s, 5H, C_5H_5), 6.01 (D, $|^2J(PH)+{}^4J(PH)|$ = 32.84 Hz, H_α), 7.50–7.85 (m, 10H, Ph). $^{13}C\{^1H\}$ NMR (CD_3NO_2): δ 18.28 (D, $|^3J(PC)+{}^5J(PC)|$ = 14.51 Hz, β-CH_3), 22.06 (s, 2-CH_3), 52.18 (dd, $^1J(PC)$ = 32.42 Hz, $^3J(PC)$ = 10.66 Hz, C_1). 67.31 (D, $|^2J(PC)+{}^4J(PC)|$ = 7.48 Hz, C_2), 88.56 (s, C_5H_5), 125.72 (D, $|^1J(PC)+{}^3J(PC)|$ = 49.65 Hz, C_α, 130.31 (D, $|^3J(PC)+{}^5J(PC)|$ = 11.26 Hz, C_m), 133.24 (s, C_p), 134.10 (D, $|^2J(PC)+{}^4J(PC)|$ = 12.85 Hz, C_o), 135.71 (dd, $^1J(PC)$ = 46.33 Hz, $^3J(PC)$ = 1.81 Hz, C_i), 161.00 (D, $|^2J(PC)+{}^4J(PC)|$ = 9.37 Hz, C_β, 200.38 (t, $^2J(PC)$ = 17.15 Hz, CO). Anal. Found: C, 50.14; H, 4.40. $C_{30}H_{31}F_6OP_3Ru$ Calc.: C, 50.36; H, 4.37%. **3a** and **3b**: the [4 + 2] cycloadducts were not further separated and were only characterized by $^{31}P\{^1H\}$ NMR ($CDCl_3$). **3a**: δ 68.20 (d, $^2J(PP)$ = 39.06 Hz, 1P, P_2), 159.86 (d, $^2J(PP)$ = 39.06 Hz, 1P, P_7), −144.95 (septet, $^1J(PF)$ = 713 Hz, 1P, PF_6^-). **3b**: 66.55 (d, $^2J(PP)$ = 31.74 Hz, 1P, P_2), 156.35 (d, $^2J(PP)$ = 31.74 Hz, 1P, P_7), −144.95 (septet, $^1J(PF)$ = 713 Hz, 1P, PF_6^-).

4.3.2. $L = PhN\equiv C$

In the same manner as above, after photolysis for 10 h, three products were formed from 0.15 g of $[(\eta^5\text{-}C_5H_5)Ru(DMPP)_2(PhNC))]PF_6^-$, **2b**, **4a** and **4b** in an 8:2:1 ratio. **2b** was isolated as a white crystalline solid (0.10 g, 66.7%); m.p. 250–251 °C. IR (KBr): ν_{CN} 2115, $\nu_{(C_5H_5 \text{ and } PF_6^-)}$ 850 cm^{-1}. $^{31}P\{^1H\}$ NMR ($CDCl_3$): δ 106.34 (s, 2P, DMPP [2 + 2]), −144.95 (septet, $^1J(PF)$ = 713 Hz, 1P, PF_6^-). ^1H NMR ($CDCl_3$): δ 1.61 (s, 6H, 2-CH_3), 1.97 (s, 6H, β-CH_3), 2.94 (m, $|^2J(PH)+{}^4J(PH)|$ = 17.41 Hz, 2H, H_1), 5.34 (s, 5H, C_5H_5), 6.01 (D, $|^2J(PH)+{}^4J(PH)|$ = 32.46 Hz, 2H, H_α, 7.50–7.85 (m, 15H, Ph). $^{13}C\{^1H\}$ NMR ($CDCl_3$): δ 17.82 (dd, $^3J(PC)$ = 11.55, $^5J(PC)$ = 3.77 Hz, β-CH_3), 21.98 (s, 2-CH_3), 50.72 (5L, $^1J(PC)$ = 31.42, $^3J(PC)$ = 11.76, $^2J(PP)$ = 3.88 Hz, C_1), 65.00 (dd, $^2J(PC)$ = 5.96, $^4J(PC)$ = 2.08 Hz, C_2), 84.84 (s, C_5H_5), 125.33 (s, C_i, C'_o), 125.97 (D, $|^1J(PC)+{}^3J(PC)|$ = 48.67 Hz, C_α), 128.16 (s, C'_p), 128.94 (m, $|^3J(PC)+{}^5J(PC)|$ = 11.41 Hz, C_m), 129.49 (s, C'_m), 131.58 (s, C_p), 132.60 (m, $|^2J(PC)+{}^4J(PC)|$ = 13.15 Hz, C_o), 134.81 (m, $|^1J(PC)+{}^3J(PC)|$ = 42.70 Hz, C_i), 157.53 (m, $|^2J(PC)+{}^4J(PC)|$ = 8.01 Hz, C_β), 160.74 (t, $^2J(PC)$ = 20.48 Hz, CN). The primed carbons are the phenyl carbons of PhNC. Anal. Found: C, 54.45; H, 4.65. $C_{36}H_{36}F_6NP_3Ru$ Calc.: C, 54.69; H, 4.59%. **4a** and **4b**: the [4 + 2] cycloadducts were not further separated and were only characterized by $^{31}P\{^1H\}$ NMR ($CDCl_3$): **4a**: δ 68.61 (d, $^2J(PP)$ = 39.06 Hz, 1P, P_2), 165.07 (d, $^2J(PP)$ = 39.06 Hz, 1P, P_7), −144.95 (septet, $^1J(PF)$ = 713 Hz, 1P, PF_6^-); **4b**: δ 71.69 (d, $^2J(PP)$ = 39.06 Hz, 1P, P_2),

167.85 (d, ^2J(PP) = 39.06 Hz, 1P, P_7), −144.95 (septet, ^1J(PF) = 713 Hz, 1P, PF_6^-).

4.3.3. L = DMPP

This reaction was carried out in the same manner as for the synthesis of **2a** from 0.50 g of $[(\eta^5\text{-}C_5H_5)Ru(DMPP)_3]PF_6$. The reaction was complete in about 30 h to give three compounds, **2c**, **5a** and **5b** in a 3:4:1 ratio. Two other minor products, **5c** and **5d**, were observed in the $^{31}P\{^1H\}$ NMR spectrum of the reaction mixture in trace amounts [**5c**: δ 147.00 (d, ^2J(PP) = 31.39 Hz, 1P), 38.90 (d, ^2J(PP) = 31.39 Hz, 1P); **5d**: δ 99.50 (d, ^2J(PP) = 33.21 Hz, 1P), 35.20 (d, ^2J(PP) = 33.21 Hz, 1P)]. **5a**, the least soluble of these compounds, was isolated as a lemon-yellow crystalline solid in 40% yield by slow evaporation of the chloroform solution; m.p. 254–256 °C. **2c** was subsequently isolated from the filtrate as a pale yellow solid in 20% yield; m.p. 154–160 °C. $^{31}P\{^1H\}$ NMR ($CDCl_3$): **2c**: δ 42.66 (t, ^2J(PP) = 39.53 Hz, 1P, DMPP), 106.32 (d, ^2J(PP) = 39.53 Hz, 2P, DMPP [2 + 2]), −144.95 (septet, ^1J(PF) = 713 Hz, 1P, PF_6^-); **5a**: δ 47.95 (dd, ^{2}J(PP) = 34.37, 25.19 Hz, 1P, DMPP), 72.01 (dd, ^2J(PP) = 48.85, 25.19 Hz, 1P, P_2), 166.52 (dd, ^2J(PP) = 48.85, 34.37 Hz, 1P, P_7), −144.95 (septet, ^1J(PF) = 713 Hz, 1P, PF_6^-); **5b**: δ 44.46 (dd, ^2J(PP) = 36.13, 28.83 Hz, 1P, DMPP), 66.83 (dd, ^2J(PP) = 41.85, 28.83 Hz, 1P, P_2), 175.10 (dd, ^2J(PP) = 41.85, 36.13 Hz, P_7), −144.95 (septet, ^1J(PF) = 713 Hz, 1P, PF_6^-). ^{1}H NMR: **2c** ($CDCl_3$): δ 1.46 (s, 6H, 2-CH_3), 1.63 (s, 6H, β′-CH_3), 1.68 (s, 6H, β-CH_3), 3.26 (m, H_1), 5.22 (s, C_5H_5), 5.62 (d, ^2J(PH) = 31.56, 2H, H_α), 6.00 (D, $|^2J(PH) + {}^4J(PH)|$ = 35.76 Hz, 2H, H'_α), 6.50–7.60 (m, 15H, PPh); **5a** (CD_3NO_2): δ 1.09 (s, 3H, 7-CH_3), 1.40 (d, ^4J(HH) = 0.9 Hz, 3H, 6-CH_3), 1.89 (d, ^4J(PH) = 0.9 Hz, 3H, 9- or 10-CH_3), 1.96 (apparent t, d, $^4J(HH) = {}^4J(PH)$, ^4J(HH) = 1.2 Hz, 3H, β-CH_3), 2.18 (apparent t, $^4J(HH) = {}^4J(PH)$ = 1.2 Hz, 3H, β-CH_3), 2.40 (d, ^4J(PH) = 0.9 Hz, 3H, 9- or 10-CH_3), 2.69 (dd, ^2J(PH) = 1.8, ^4J(HH) = 1.8 Hz, 1H, H_3), 2.93 (apparent dt, ^3J(PH) = 47.18, $^2J(PH) = {}^3J(HH)$ = 4.21 Hz, 1H, H_2), 3.41 (ddd, ^2J(PH) = 3.91, ^3J(PH) = 3.31, ^4J(HH) = 1.8 Hz, 1H, H_1), 4.68 (s, 5H, C_5H_5), 5.63 (dq, ^2J(PH) = 32.16, ^4J(HH) = 1.20 Hz, 1H, H_5), 6.43 (d, ^2J(PH) = 35.76 Hz, 1H, H'_α), 6.58 (d, ^2J(PH) = 33.96 Hz, 1H, H_α), 7.10–7.70 (m, 15H, Ph). $^{13}C\{^1H\}$ NMR: **2c** ($CDCl_3$): δ 16.39 (d, ^3J(PC) = 12.30 Hz, β′-CH_3), 17.29 (m, $|^3J(PC) + {}^5J(PC)|$ = 13.00 Hz, β-CH_3), 21.10 (s, 2-CH_3), 47.29 (m, $|^1J(PC) + {}^3J(PC)|$ = 42.63 Hz, C_1), 64.07 (s, C_2), 82.68 (s, C_5H_5), 125.87 (D, $|^1J(PC) + {}^3J(PC)|$ = 49.50 Hz, C_α), 127.65 (d, ^3J(PC) = 10.05 Hz, C'_m), 128.41 (T, $|^3J(PC) + {}^5J(PC)|$ = 9.83 Hz, C_m), 128.55 (s, C'_p), 129.03 (d, ^1J(PC) = 45.35 Hz, C'_α), 129.87 (s, C_p), 130.56 (d, ^2J(PC) = 10.43 Hz, C'_o,), 130.99 (T, $|^2J(PC) + {}^4J(PC)|$ = 10.88 Hz, C_o), 133.55 (m, C'_i), 134.13 (m, C_i), 149.24 (d, ^2J(PC) = 9.30 Hz, C'_β), 152.19 (T, $|^2J(PC) + {}^4J(PC)|$ = 7.18 Hz, C_β); **5a**: (CD_3NO_2): δ 15.42 (s, 9- or 10-CH_3), 17.10 (d, ^3J(PC) = 12.01 Hz, β-CH_3), 17.18 (s, 9- or 10-CH_3), 18.78 (d, ^3J(PC) = 14.44 Hz, 6-CH_3), 26.79 (d, ^3J(PC) = 5.74 Hz, 7-CH_3), 50.02 (dd, ^1J(PC) = 35.98, ^2J(PC) = 32.42 Hz, C_3), 57.28 (dd, ^1J(PC) = 35.98, ^2J(PC) = 32.42 Hz, C_2), 61.90 (dd, ^1J(PC) = 18.71, ^2J(PC) = 6.14 Hz, C_2), 64.10 (dd, ^1J(PC) = 15.34, ^3J(PC) = 2.30 Hz, C_8), 84.84 (q, ^2J(PC) = 1.13 Hz, C_5H_5), 126.95 (dd, ^1J(PC) = 51.24, ^3J(PC) = 6.50 Hz, C_5), 129.59 (d, ^3J(PC) = 9.15 Hz, C'_m), 130.13 (d, ^3J(PC) = 10.51 Hz, C_m), 130.54 (d, ^3J(PC) = 10.43 Hz, C_m), 130.60 (d, ^2J(PC) = 12.77 Hz, C_o), 130.69 (d, ^4J(PC) = 1.74 Hz, C'_p), 131.11 (d, ^2J(PC) = 9.45 Hz, C_o), 131.20 (dd, ^1J(PC) = 51.24, ^3J(PC) = 2.72 Hz, C'_α), 131.67 (d, ^4J(PC) = 2.65 Hz, C_p), 132.02 (d, ^4J(PC) = 2.49 Hz, C_p), 133.44 (d, ^2J(PC) = 13.08 Hz, C_o), 134.40 (d, ^1J(PC) = 34.16, C'_i), 135.15 (d, ^1J(PC) = 48.29 Hz, C'_α), 135.47 (s, C_5 or C_6), 137.56 (s, C_9 or C_{10}), 138.64 (m, C_i), 140.17 (dd, ^1J(PC) = 37.41, ^3J(PC) = 6.05 Hz, C_i), 148.08 (d, ^2J(PC) = 8.69 Hz, C_6), 153.45 (d, ^2J(PC) = 9.83 Hz, C'_β), 154.60 (d, ^2J(PC) = 16.02 Hz, C'_β). The primed nuclei are the phosphole nuclei. Anal. Found: **2c**: C, 56.37; H, 5.29. **5a**: C, 56.25; H, 5.25. $C_{41}H_{44}F_6P_4Ru$ Calc.: C, 56.25; H, 5.02%.

4.4. Photolysis of $[(\eta^5\text{-}C_5H_5)Ru(DMPP)_2\text{-}[(CH_3O)_3P]]PF_6$

When a solution of this complex, 0.50 g in $CHCl_3$, was subjected to sunlight, intramolecular [4 + 2] and [2 + 2] cycloadditions occurred. The reaction was complete in about 40 h to give three compounds, **2f**, **6a** and **6b** in a 6:1:1 ratio. In addition there were trace amounts of unidentified products. The compounds were characterized only by $^{31}P\{^1H\}$ NMR ($CDCl_3$): **2f**: δ 149.05 (t, ^2J(PP) = 61.48 Hz, 1P, $(CH_3O)_3P$), 105.95 (d, ^2J(PP) = 61.48 Hz, 2P, DMPP [2 + 2]), −144.95 (septet, ^1J(PF) = 713 Hz, 1P, PF_6^-); **6a**: δ 174.46 (dd, ^2J(PP) = 53.77, 32.96 Hz, 1P, P_7), 153.31 (dd, ^2J(PP) = 53.77, 50.98 Hz, 1P, $(CH_3O)_3P$), 71.60 (dd, ^2J(PP) = 50.98, 32.96 Hz, 1P, P_2), −144.95 (septet, ^1J(PF) = 713 Hz, 1P, PF_6^-); **6b**: δ 172.02 (dd, ^2J(PP) = 40.81, 36.86 Hz, 1P, P_7), 159.09 (dd, ^2J(PP) = 54.80, 36.86 Hz, 1P, $(CH_3O)_3P$, 66.95 (dd, ^2J(PP) = 40.81, 54.80 Hz, 1P, P_2), −144.95 (septet, ^1J(PF) = 713 Hz, 1P, PF_6^-).

4.5. Reaction mechanism studies

Solid **2a** (0.38 g) was sealed in an ampoule under N_2 and heated in an oven at 100 °C for 24 h. A color change from shiny white to pale yellow occurred. The $^{31}P\{^1H\}$ NMR spectrum ($CDCl_3$) showed that no change had occurred, the [2 + 2] cycloadduct remained, and was recovered by recrystallization. Similarly, a solution in 1,1,2,2-tetrachloroethane was heated at reflux for

10 h under N_2 and a darkening in color was observed. However, the $^{31}P\{^1H\}$ NMR spectrum of this solution indicated that neither conversion to the [4 + 2] adduct nor decomposition had occurred to any noticeable extent. The [2 + 2] cycloadduct was recovered by addition of diethyl ether. In a similar fashion **2b** did not convert to **4a** or **4b**. A solution of $[(\eta^5\text{-}C_5H_5)Ru(DMPP)_3]PF_6$ in dry $CHCl_3$ was heated at reflux in the dark overnight, and the complex was recovered unchanged by addition of diethyl ether. The $[(\eta^5\text{-}C_5H_5)Ru(DMPP)_2L]PF_6$ complexes, L = CH_3CN, Ph_3P, $PhS(O)_2CH{=}CH_2$, $P(C{\equiv}CPh)_3$ and Cl were dissolved in chloroform and the solutions exposed to sunlight for 10 days. The $^{31}P\{^1H\}$ NMR spectra of each of these solutions showed that no cycloadditions had occurred.

4.6. X-ray data collection and processing

Suitable colorless crystals of **2a** were obtained by slow evaporation of a $CH_2Cl_2/CHCl_3$ solution at ambient temperature. A systematic search in reciprocal space using a single crystal cut out from a cluster of crystals on an Enraf–Nonius CAD4-F automatic diffractometer showed that they belong to the monoclinic system. Quantitative data were obtained at room temperature. The resulting data set was transferred from the instrument computer to a VAX computer, and for all subsequent calculations the Enraf–Nonius SDPfVAX package [25] was used. Three standard reflections measured every hour during the entire data collection period showed no significant trend. The raw data were converted to intensities and corrected for Lorentz and polarization factors.

The structure was solved by the heavy atom method. After refinement of the non-hydrogen atoms, a difference-Fourier map revealed maxima of residual electronic density close to the positions expected for the hydrogen atoms; they were introduced in the structure factor calculations by their computed coordinates (CH = 0.95 Å) with isotropic temperature factors such as $B(H) = 1.3B$ eqv (C) Å, but were not refined. At this stage empirical absorption corrections were applied using the method of Walker and Stuart [26]. Full least-squares refinements minimizing $\Sigma w(|F_o| - |F_c|)^2$ with $\sigma^2(F)^2 = \sigma^2$ counts + $(pI)^2$ converged to the values given in Table 6. A final difference map revealed no significant maxima. The scattering factor coefficients and anomalous dispersion coefficients come respectively from Refs. [27,28]. Further details of the crystal structure investigation are available from either J.H. Nelson or J. Fischer.

Table 6
Crystallographic data for **2a**

chemical formula	$C_{30}H_{31}F_6OP_3Ru \cdot 2CH_2Cl_2$
FW	885.4
a (Å)	28.611(8)
b (Å)	11.564(3)
c (Å)	11.587(3)
β (°)	101.08(2)
V (Å^3)	3762.2
Z	4
space group	$P2_1/n$
T (°C)	20
λ (Å)	0.7093
ρ_{calc} (g cm^{-3})	1.563
μ (cm^{-1})	8.751
abs. min/max	0.89/1.08
$R(F)$ [a]	0.054
$R_w(F)$	0.081

[a] Minimizing $\Sigma w(|F_o| - |F_c|)^2$ with $\sigma^2(F)^2 = \sigma^2(\text{counts}) + (pI)^2$.

Acknowledgements

We are grateful to the donors of the Petroleum Research Fund, administered by the American Chemical Society, for financial support, and to Johnson Matthey Aesar/Alfa for their generous loan of ruthenium.

References

[1] C.C. Santini, J. Fischer, F. Mathey and A. Mitschler, *J. Am. Chem. Soc.*, *102* (1980) 5809.
[2] D.G. Holah, A.N. Hughes and D. Kleemola, *J. Heterocycl. Chem.*, *14* (1971) 705; T.H. Chan and L.T. Wang, *Can. J. Chem.*, *49* (1971) 530; D.J. Collins, L.E. Rowley and J.M. Swan, *Aust. J. Chem.*, *27* (1974) 831.
[3] H.-L. Ji, J.H. Nelson, A. DeCian, J. Fischer, L. Solujic' and E.B. Milosavljevic', *Organometallics*, *11* (1992) 1840.
[4] P.E. Garrou, *Chem. Rev.*, *81* (1981) 229.
[5] L.D. Quin and K.A. Mesh, *Org. Magn. Reson.*, *12* (1979) 442.
[6] D.A. Redfield, L.W. Cary and J.H. Nelson, *Inorg. Chem.*, *14* (1975) 50; D.A. Redfield, J.H. Nelson and L.W. Cary, *Inorg. Nucl. Chem. Lett.*, *10* (1974) 727.
[7] H.-L. Ji, J.H. Nelson, A. DeCian, J. Fischer, L. Solujic' and E.B. Milosavljevic', *Organometallics*, *11* (1992) 401.
[8] W. Carruthers, *Cycloaddition Reactions in Organic Synthesis*, Pergamon, New York, 1990.
[9] G. Consiglio and F. Morandini, *Chem. Rev.*, *87* (1987) 761.
[10] K. Stanley and M.C. Baird, *J. Am. Chem. Soc.*, *97* (1975) 6598; T.E. Sloan, *Top. Stereochem.*, *12* (1981) 1.
[11] J.H. Nelson, *Coord. Chem. Rev.*, *139* (1995) 245.
[12] R.E. Stanton and J.W. McIver, Jr., *J. Am. Chem. Soc.*, *97* (1975) 3632.
[13] T.H. Peterson and B.K. Carpenter, *J. Am. Chem. Soc.*, *114* (1992) 1496.
[14] P.J. Kropp, in A. Padwa (ed.), *Organic Photochemistry*, Vol. 4, Marcel Dekker, New York, 1979; A. Gilbert, in W.M. Horspool (ed.), *Synthetic Organic Photochemistry*, Plenum Press, New York, 1984; J.J. McCullough, *Chem. Rev.*, *87* (1987) 811.
[15] F.C. DeSchryver, N. Boems, J. Huybrechts, J. Daemen and M. Brackelaire, *Pure Appl. Chem.*, *49* (1977) 237.
[16] D. Catheline and D. Astruc, *J. Organomet. Chem.*, *248* (1983) C9.

[17] W.L. Wilson, J.A. Rahn, N.W. Alcock, J. Fischer, J.H. Frederick and J.H. Nelson, *Inorg. Chem.*, *33* (1994) 109.
[18] W.L. Wilson, J. Fischer, R.E. Wasylishen, K. Eichele, V.J. Catalano, J.H. Frederick and J.H. Nelson, *Inorg. Chem.*, *35* (1996) 1486.
[19] G.A. Crosby, in R.B. King (ed.), *Advances in Chemistry*, ACS Monograph Series 150, American Chemical Society, Washington, DC, 1976, pp. 149–159.
[20] N.J. Turro, *Modern Molecular Photochemistry*, Benjamin/Cummings, Menlo Park, CA, 1978, pp. 419 ff.
[21] G. Condorelli, L. Giallongo, A. Giuffrida and G. Romeo, *Inorg. Chim. Acta*, *7* (1973) 7; Y. Yamamoto, T. Tanese, T. Date and Y. Koide, *J. Organomet. Chem.*, *386* (1990) 365; D.E. Bursten and M.R. Green, *Progr. Inorg. Chem.*, *36* (1988) 393.
[22] E.B. Milosavljevic', L. Solujic', D.W. Krassowki and J.H. Nelson, *J. Organomet. Chem.*, *352* (1988) 177.
[23] R.A. Appel, R. Kelinstuck and K.-D. Ziehn, *Angew. Chem., Int. Ed. Engl.*, *10* (1971) 132.
[24] J.H. Nelson, W.L. Wilson, L.W. Cary, N.W. Alcock, H.J. Clase, G.S. Jas, L. Ramsey-Tassin and J.W. Kenney, III, *Inorg. Chem.*, *35* (1996) 883.
[25] B.A. Frenz, in H. Schenck, R. Olthof-Hazekamp, H. Van Koningsveld and G.C. Bassi (eds.), *Computing in Crystallography*, Delft University Press, Delft, Netherlands, 1978, pp. 64–71.
[26] N. Walker and D. Stuart, *Acta Crystallogr., A39* (1983) 158.
[27] D.T. Cromer and J.T. Walker, *International Tables for X-ray Crystallography*, Kynoch Press, Birmingham, UK, 1974, Table 2.2b.
[28] D.T. Cromer and J.T. Walker, *International Tables for X-ray Crystallography*, Kynoch Press, Birmingham, UK, 1974, Table 2.3.1.